Analysis of the effect of the operational variants in a combined adsorption-ozonation process with granular activated carbon for the treatment of phenol wastewater

Cristian Ferreiro,*[a] Natalia Villota,[b] Ana de Luis[c] and Jose Ignacio Lombraña[a]

This work proposes a mathematical model as a basis for studying the combined adsorption-ozonation process (Ad/Ox) with the complexity involved in a three-phase system. The description of this operation involves several parameters that describe system kinetic and adsorption phenomena. This paper analyses the Ad/Ox process compared with simple ozonation, investigating the benefit of activated carbon (AC) in ozonation, primary degradation and mineralization of phenol solutions. The study focuses on Ad/Ox with granular activated carbon (GAC) and analyses how the phenol degradation kinetics depend on the amount of AC. Thus, a priority order of relevance is established for the proposed mathematical model parameters. For example, the adsorption kinetic constant may vary meaningfully within the same process. Finally, the paper studies the GAC behaviour after a given number of cycles, followed by the regeneration process. The calculated kinetic coefficients relating to the liquid and solid media explain the changes in process efficiency.

1. Introduction

It is difficult to degrade certain organic compounds, such as phenol. Phenol is chosen in this work to study the ozonation process, which has been used as a possible alternative for several decades.[1,2] Phenol is mainly used to produce phenolic resins, which are used in plywood manufacturing. It is also used in household appliance manufacturing, as well as in the production of caprolactam and bisphenol A, two intermediates used in manufacturing nylon and epoxy resins.[3,4]

Phenol is highly irritating to human skin, eyes and mucous membranes after prolonged exposure. Short-term inhalation may cause anorexia, diarrhoea, dizziness, and dark-coloured urine. Long-term effects in the blood and liver may occur. The lethal dose in humans may be as low as 14–214 mg phenol/kg.[5] The United States Environmental Protection Agency (US EPA) has classified phenol as a Group D contaminant, not classifiable with respect to human carcinogenicity.[6] However, the European Union (EU) through the European Chemicals Agency (ECHA) included this pollutant in 2015 in the Community Rolling Action Plan (CoRAP), because it is considered a suspect mutagenic substance and a potential endocrine disruptor.[7] In addition to the human health effects, it can cause considerable damage to the aquatic environment. For example, 1500 mg L^{-1} of phenol was lethal to *Chilomonas* and *Euglena gracilis*; at 2500 mg L^{-1} it was lethal to *Peramena*. At a dose of 10-40 mg L^{-1} of phenol inhibited the photosynthesis of *Chlorella*. An exposure of 50 mg L^{-1} caused *Pimephales promelas* to lose balance and gasp at the surface, while a dose of 6.3 mg L^{-1} caused hyperactivity and rapid operculation in *Salmo gairdneri*. The most critical sublethal effect of phenol is on the reproductive potential of the biota. For example, an exposure of 5 mg L^{-1} of phenol causes reduced fertility in *Daphnia longispina*.[8]

Several authors noted in the bibliography studied the elimination of phenol from industrial wastewater, as shown in Table 1. The processes studied to date require complex treatment and reaction times large enough to achieve complete degradation and a sufficiently high degree of mineralization to avoid damage to the environment. Therefore, the ozonisation process is proposed as a clear alternative for the elimination of phenol. Nevertheless, the unstable character of ozone makes its effective application complicated, as demonstrated in several studies within recent decades.[9–11] This disadvantage leads us to consider the convenience of combining ozonation with catalysts and adsorbent materials such as activated carbon (AC).

In early attempts to add active carbon in ozonation, the benefits were connected to the high adsorption capacity of AC.[12] Subsequent studies[13–15] have shown that AC catalyses the decomposition of ozone in the aqueous phase by accelerating the transformation of free hydroxyl radicals. Generally, ozone is adsorbed on the surface of the AC at acidic pH values, but the generation of hydroxyl radicals is minimal by this route, since the predominant mechanism is the molecular path. However, at a pH between 6-9, ozone decomposition occurs and is catalysed by hydroxyl groups adsorbed onto AC surface.[16] The mechanism of ozone decomposition and the subsequent phenol oxidation in the presence of activated carbon is shown below:[2]

$$O_3 \xrightarrow{OH^-} {}^{\bullet}OH \qquad (1)$$

$$AC + Phenol \rightarrow AC\text{-}Phenol \qquad (2)$$

$$O_3 \xrightarrow{AC} {}^{\bullet}OH \quad (3)$$

$${}^{\bullet}OH + \text{Phenol} \rightarrow \text{Oxidationproducts} \quad (4)$$

$$O_3 + AC \rightarrow AC\text{-}O \quad (5)$$

$$AC\text{-}O + AC\text{-Phenol} \rightarrow \text{Oxidation products} \quad (6)$$

$$AC\text{-Phenol} + O_3 \rightarrow \text{Oxidation products} \quad (7)$$

$$AC\text{-Phenol} + {}^{\bullet}OH \rightarrow \text{Oxidation products} \quad (8)$$

Later, Beltran et al. and Sanchez et al. concluded that with these processes, the complete mineralization of many pollutants is possible.[17,18] These authors studied O_3/AC systems in detail and showed that the surface chemistry of activated carbon, along with its textural characteristics, plays a very important role in its behaviour as promoter of ozone decomposition to hydroxyl radicals.

Ozonation combined with AC can operate in a batch process, but it is generally sequential, which presents disadvantages in application.[24–26] In this work, the simultaneous application of adsorption and ozonisation is proposed, analysing the elimination of phenol as a pollutant.[27] AC's application together with ozonation occupies a relevant place in recent works for its clear advantages in catalytic heterogeneous ozonation. The increasing development of new activated carbons,[28,29] and the advantages associated with their dual functions (adsorptive and catalytic) support the growth of this technology.[30,31]

Despite the findings in this field,[32,33] it is necessary to detail the combined action of ozone and activated carbon to predict and estimate the effects of the process and operational variants on the removal performance. In this respect, this work contributes with suitable modelling and estimation of the characteristic parameters of the combined system and their influence on the process efficiency.

Table 1 Previous studies on the treatment of industrial wastewater containing phenol.

Treatment	Catalyst	Operation Conditions	Comments	References
Noncatalytic wet air oxidation	—	[*T*]=125-320°C; [*P*]=0.5-20 MPa [Time]=120 min [% COD]=75-90%; Acidic media	Extremely clean process because it neither uses any harmful chemical reagents nor produces any harmful final products (carbon dioxide and water are the products if a complete oxidation is achieved).	19
TiO_2/UV photocatalysis	TiO_2	[Cat] =1 g L^{-1}; C_0=50 mg L^{-1} [Time]=90 min [UV power]=400 W [%]=100%; Intermediate pH	The oxidation of phenol under UV irradiation and the presence of photocatalysts leads to increased degradation. The immobilization of the photocatalyst led to a reduction in photoactive capacity compared to the use of the suspended catalyst.	20
Microwave in UV/H_2O_2 system	—	[MW irradiation]=2.5 GHz [% TOC]=50%; C_0=200 mg L^{-1} [H_2O_2]=1200 mg L^{-1} *T*=50°C; [%]=95% [Time]=30 min	The introduction of microwave irradiation into the system reduces reaction times, increases reaction selectivity, reduces activation energy, reduces equipment size and makes the process easier to control.	21
Fenton reaction	Fe/ZrO_2 and 4% Fe-sulfonated-ZrO_2	C_0=0.1 g L^{-1}; [H_2O_2]=0.5 g L^{-1} [Cat]=2 g L^{-1}; *T*=25°C *P*=1 atm; [Time]=6 h [%]=100%; [% TOC]=64% Acidic media	Sulfonation of zirconia followed by Fe impregnation shows a positive effect on the oxidative degradation and mineralization of phenol. The catalyst maintains its activity even after four cycles of regeneration and reuse.	22
O_3/$Ca(OH)_2$	$Ca(OH)_2$	C_0=450 mg L^{-1}; [Cat]=2 g L^{-1} $C_{O_3,G}$=75 mg L^{-1}; Q_G=3 L min^{-1} *T*=25°C; *P*=0.25 MPa [Time]=55 min; [%]=100% [% TOC]=100%	It is necessary to treat the catalyst as a solid residue once spent. The mechanism for $Ca(OH)_2$ intensified mineralization of phenol solution is the simultaneous removal of CO_3 2-ions, as hydroxyl radical scavengers, due to the presence of Ca^{2+} ions.	4
O_3/Cu-AC	Cu-AC	C_0=200 mg L^{-1} [Cat]=2.5 mg mL^{-1} $C_{O_3,G}$=11.2 mg L^{-1}; pH_0=4 *T*=25°C; *P*=1 atm [Time]=30 min; [%]=70%	The presence of the Cu-AC catalyst enhances the decomposition of ozone into hydroxyl radicals. The CuO and surface oxygen groups in the activated carbon have a slight effect on the degradation of phenol.	23

This study analyses the results obtained when using granular activated carbon (GAC) during ozonation. Based on an adsorption study of active carbon with solutions containing phenol, the simultaneous mode of operation (Ad/Ox) was studied, using the advantages of the adsorptive-reactive function that occurs on the AC surface. The study objective is therefore to assess the extent of the adsorption and reaction effect in the efficiency of phenol removal, used here as a pollutant model, considering catalytic material regeneration.

2. Experimental methods

2.1. Materials and reagents

Phenol (C_6H_5OH, Sigma-Aldrich, ≥99.0%), sulfuric acid (H_2SO_4, Panreac, 1 M), sodium hydroxide (NaOH, Panreac, 1 M), hydrogen chloride (HCl, Labkem, 37%), sodium chloride (NaCl, VWR, 99.8%), powder activated carbon (PAC, Panreac, pure) and HPLC-grade methanol (CH_3OH, Merck, >99.99%) were used as received. Deionised water was supplied by a Milli-Q® water purification unit supplied by Merck. Kemisorb® 530 GR 12x40 granular activated carbon was purchased from Kemira.

2.2. GAC characterization methods

Nitrogen adsorption measurements were performed using the Micromeritics ASAP 2010 instrument at 77 K with ultra-high purity nitrogen gas. All samples were dried and degassed under high vacuum at 473 K for 24 h prior to measurement. The surface area was calculated using the BET equation, and the pore size distribution was determined by applying the BJH model.

The point of zero charge (PZC) was determined by the acid-base titration method.[34,35] A total of 50 mL of 0.01 M NaCl solution was prepared in 100-mL flasks. The initial pH between 2 and 12 was then adjusted using 0.1 M NaOH or HCl, and then, 0.15 g of activated carbon was added to start the test at a certain pH. After a 24-h contact time, the final pH was measured. The final pH was plotted against the initial pH for all assays to obtain the pH_{pzc} value.

A Waters 2695 HPLC system with a Teknokroma Mediterranea SEA C18 threaded column (150 mm x 4.6 mm, 1.8 µm) with the guard column working at 20°C under isocratic elution (60% buffered water at pH 3, 40% methanol) and a flow rate of 1 mL min^{-1} was used for phenol quantification. A Waters 2487 UV/Vis detector was used at a wavelength of 272 nm. The degree of mineralization was quantified by total organic carbon (TOC) analysis in a Shimadzu TOC-VSCH Analyzer.

2.3. Adsorption experiments

Phenol adsorption experiments on activated carbon were performed at temperatures ranging from 15-35°C and at 6.5 pH for powdered active carbon and for granular activated carbon, Kemisorb® 530. The kinetics and adsorption isotherms were obtained by preparing 500.0 mL phenol solutions, in a 0.5 L jacketed reactor with a magnetic stirrer, in which 0.25 g of carbon active powder or granulate were added, after adjusting the pH according to the experiment.

The agitation was kept steady at 500 rpm, in order to maintain perfect mixing for at least 24 h, to assure equilibrium. The temperature was controlled by a thermostatic bath, providing the reactor with necessary water flux at the desired temperature. To remove the catalyst particles, the solutions were filtered through a 0.45-µm membrane (MF-Millipore) before proceeding to the analysis of the concentration of phenol by HPLC. For equilibrium data, the amount of phenol adsorbed onto the activated carbon q_∞ (mg g^{-1}), was calculated through Eq. 9:

$$q_\infty = \frac{(C_0 - C_\infty)\cdot V}{M} \quad (9)$$

where C_0 and C_∞ are the initial and equilibrium phenol concentrations, respectively; V is the volume of the solution and M is the mass of activated carbon. For the analysis of adsorption kinetic data, the amount of phenol adsorbed at time t was obtained from Eq. 10:

$$q_t = \frac{(C_0 - C_t)\cdot V}{M} \quad (10)$$

where C_t is the phenol concentration at any time. All adsorption experiments were performed in triplicate, and the mean values were used for the adsorption study. The maximum standard deviation of measured concentrations was no greater than 0.1 mg L^{-1}.

2.4. Ozonation experiments

The removal of phenol in the Ad/Ox process was carried out in a gas-liquid contactor using powder activated carbon and, in other cases, granular activated carbon Kemisorb® 530. The experimental ozonation system consisted of a 30.41-L cylindrical column where the solution to treat was placed. Ozone gas is introduced into the reactor through a venturi installed in the recirculation stream, thus ensuring a perfect homogenization of the system. To improve the contact between the descending liquid and the ascending gas, the column has a sprayer on the top that atomizes the liquid (Fig. 1). Part of the solution that the system recirculates is pumped upward and returns to the reactor at the top, where it is sprayed, thus destroying foam that is formed in some cases by the strong agitation of the system. The recirculation system provides enough stirring to ensure a good mixture in the system. As shown in Fig. 1, the reacting medium interacts with a certain load of GAC packed in a cartridge, through which the reacting stream passes.

The experiments were carried out at a constant temperature of 20.0°C, operated in batches with loads of approximately 10.0 L of phenol solutions at different concentrations. All assays were carried out under constant gas flow, Q_G=4.0 L min^{-1}, constant ozone concentration in gas phase at the inlet, $C_{O_3,G}$=19.0 mg L^{-1}, a pH of 6.5 and 250.0 or 500.0 g of activated carbon. Ozone was produced from extra pure oxygen in the TRIOGEN LAB2B generator. The temperature was controlled using a refrigerating bath. The ozone concentration in the gas phase was monitored with a BMT 964C ozone analyser. The ozone concentration in the liquid phase and temperature were measured with a Rosemount Analytical model 499AOZ-54 probe inserted in the conduction (top) of the recirculating liquid. The pH was controlled with a Rosemount Analytical model 399-09-62 probe, integrated with the ozone probe in a Rosemount Analytical Solu Comp II recorder. Gas-phase ozone leaving the reactor was removed with a Zonosistem thermocatalytic ozone destructor.

2.5. GAC regeneration

2.5.1. Regeneration with NaOH

The regeneration of granulated activated carbon was carried out according to the procedure described by Martin & Ng and Sun et al.,[36,37] which consists of treating spent activated carbon with a 10% NaOH solution at a temperature of 105°C, circulating in the opposite direction as that during the reaction. The activated carbon was then washed with distilled water to neutralize its pH before drying in an oven at 90°C for 24 hours.

2.5.2. Ozone regeneration procedure

In this case, spent granular activated carbon was treated according to the procedure described by He et al. (2017), which consists of placing the spent GAC into a jacket glass reactor with 1500 mL of deionized water, similar to the process described by Ferreiro et al.[28] An ozone gas flow, Q_G=4.0 L min^{-1}, was then introduced, using an ozone concentration of 262.0 mg O_3/g GAC treated.[39] The GAC was treated with ozone for 60 min. and then dried in an oven at 90°C for 24 h before reuse.

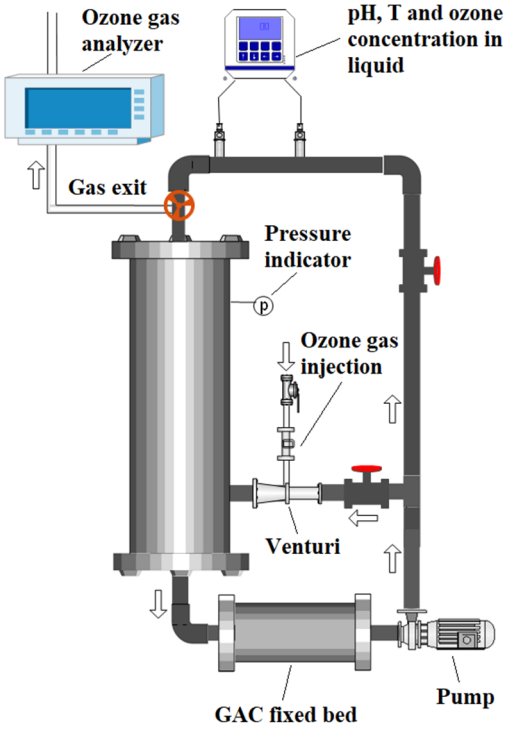

Fig. 1 Diagram of the Ad/Ox experimental equipment used to carry out ozonation assays with phenol.

3. Theory

3.1. Three-phase reaction model

As described in the introduction, a combined Ad/Ox process is postulated as a good option for the treatment of contaminants such as phenol. In this section, a mathematical model is proposed to describe the simultaneous ozonisation and adsorption process (Ad/Ox), in batch, based on the definition of the corresponding adsorption and phenol oxidation kinetic constants. The proposed model calculates the variation in the phenol concentration during the reaction, and analyses the oxidation that takes place in the liquid and the active carbon.

Phenol's primary degradation process can be described through ozone consumption. In this case, the stoichiometric coefficient, *z*, of the reaction between phenol and ozone is used, according to:

$$-\frac{dC_P}{dt} = z \cdot N_{O_3} \qquad (11)$$

where N_{O3} is the ozone consumption, coincident with the ozone transferred to the G-L-S system. The coefficient *z* can also be thought of as the efficiency of the global ozonisation process, involving several stages of mass transfer and chemical reactions. Fig. 2 shows a resistance model of the mass transfer and chemical reaction stages involved in the global ozonation process.

According to Fig. 2, in this case, reactions occur simultaneously in the liquid and inside the activated carbon, in many cases conditioned by the ozone transfer rate through the liquid and in the solid.[40] The total consumption of ozone in the process, which occurs both in the liquid phase and within the active carbon (see the green dotted line in Fig. 2), is given by:

$$N_{O_3} = K_G^*\left(P_{O_3} - 0\right) = K_G\, a_1\left(P_{O_3} - P_{O_3}^*\right) = K_L^*\left(C_{O_3} - 0\right) = \frac{K_L^*}{He}\left(P_{O_3}^* - 0\right) \qquad (12)$$

where K_G^* is the overall ozonation process coefficient, including the material transfer and chemical reaction stages in the total parallel-series system (Fig. 2), collected through the constants K_G and K_L^*. Consequently, the ozone transfer rate, N_{O3}, is directly proportional to the driving force of the ozone partial pressure, P_{O3}.

The overall gas-liquid mass transfer coefficient, $K_G{\cdot}a_1$, can be expressed in terms of the individual liquid and gas coefficients ($k_L{\cdot}a_1$ and $k_G{\cdot}a_1$; double film theory). Thus, taking into account Henry's constant, *He*, corresponding to the G-L equilibrium, we have the following equation:

$$K_G a_1\left(P_{O_3} - P_{O_3}^*\right) = k_G a_1\left(P_{O_3} - P_{O_3,i}\right) = k_L a_1\left(C_{O_3,i} - C_{O_3}\right) = \frac{k_L}{He} a_1\left(P_{O_3,i} - P_{O_3}^*\right) \qquad (13)$$

where $P_{O3,\,i}$ is the partial pressure of ozone at the G-L interface, in equilibrium with that of the liquid interface, $C_{O3,\,i}$.

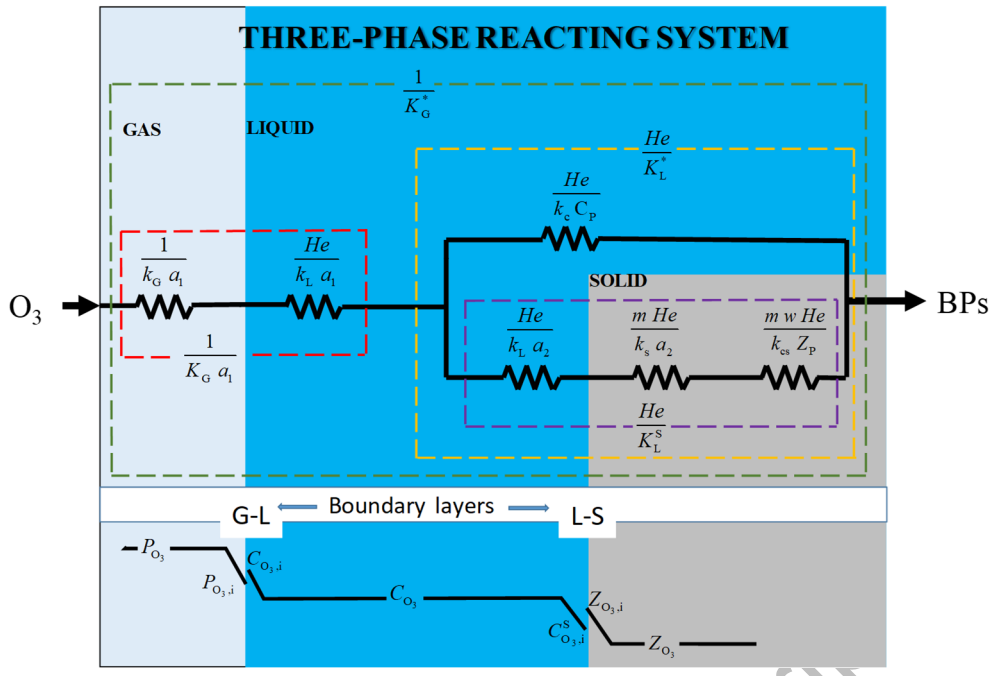

Fig. 2 Ozone transfer phenomena and chemical reaction resistances involved in the Ad/Ox process.

The ozone transferred to the liquid is consumed through the chemical reaction produced in the liquid, $N^{I}_{O_3}$(see the discontinuous blue line in Fig. 2), and through the reaction in the active carbon, $N^{II}_{O_3}$, according to the equations:

$$N^{I}_{O_3} = k_{c,L} \cdot C_{O_3} \cdot C_P = \frac{k_{c,L} \cdot C_P}{He} \cdot \left(P^{*}_{O_3} - 0\right) \quad (14)$$

$$N^{II}_{O_3} = k_{c,S} Z_{O_3} Z_P w^2 = \frac{k_{c,S} Z_P}{m}\left(C^{*}_{O_3} - 0\right) = \frac{k_{c,S} Z_P}{m\,He}\left(P^{\wedge}_{O_3} - 0\right) \quad (15)$$

Consequently, the overall ozone consumption rate, N_{O_3} (the sum of $N^{I}_{O_3}$, and $N^{II}_{O_3}$), depends on the kinetic constants indicated in Eq. 14 and 15, equalizing the ozone transferred from the gas to the liquid. Thus, $N^{I}_{O_3}$ can be expressed as a function of the diffusional parameters of ozone, by combining Eqs. 12, 13 and 14, to give:

$$N^{I}_{O_3} = \frac{\left(P_{O_3} - 0\right)}{\frac{1}{k_G a_1} + \frac{He}{k_L a_1} + \frac{He}{k_c C_P}} \quad (16)$$

The consumption of ozone in the solid, $N^{II}_{O_3}$, is described by the constant K_L^S, which includes the stages of ozone transfer and the chemical reaction inside the active carbon particles, according to:

$$K_L^S\left(C_{O_3,L} - 0\right) = k_L a_2 \left(C_{O_3} - C_{O_3,i}\right) = k_S a_2 \left(Z_{O_3,i} - Z_{O_3}\right) = k_{c,S}\left(Z_{O_3} - 0\right) \quad (17)$$

If Henry´s constant, *He*, in the equilibrium G-L is considered together with the L-S equilibrium constant, *m*, according to:

$$He = P^{*}_{O_3} / C_{O_3} = P_{O_3,i} / C_{O_3,i} = P^{\wedge}_{O_3} / C^{*}_{O_3} \quad (18)$$

$$m = C^{S}_{O_3,i} / Z_{O_3,i} = C^{*}_{O_3} / Z_{O_3}\,, \quad (19)$$

Eq. 17 can be expressed as a function of the ozone partial pressure, according to:

$$\frac{K_L^S}{He}\left(P^{*}_{O_3} - 0\right) = \frac{k_L a_2}{He}\left(P^{*}_{O_3} - P_{O_3,i}\right) = \frac{k_S a_2}{m\,He}\left(P_{O_3,i} - P^{\wedge}_{O_3}\right) = \frac{k_{c,S}}{m\,He}\left(P^{\wedge}_{O_3} - 0\right) \quad (20)$$

Consequently, $N^{II}_{O_3}$ can also be expressed as a function of the ozone transport parameters, according to:

$$N^{II}_{O_3} = \frac{\left(P_{O_3} - 0\right)}{\frac{1}{k_G a_1} + \frac{He}{k_L a_1} + \frac{He}{K_L^S}} \quad (21)$$

Moreover, the variation of phenol concentration, considering the oxidation terms in the liquid and on the surface of the active carbon, together with the removal by adsorption, gives the following general expression:

$$\left(-\frac{dC_P}{dt}\right) = \left(-\frac{dC_P}{dt}\right)_{ox,L} + \left(-\frac{dC_P}{dt}\right)_{ox,s} + \left(-\frac{dC_P}{dt}\right)_{ads} \quad (22)$$

The proposed model is based on the following assumptions:

- The liquid and solid oxidisation rates in are considered to be pseudo-first order with respect to phenol.
- The pseudo-first order constants are affected by the ozone transport parameters, which leads to certain ozone concentrations: C_{O_3} (in the liquid) and Z_{O_3} (in the solid). Both C_{O_3} and Z_{O_3} are considered constants once they have reached steady state.
- Activated carbon consists of porous particles in which ozone and phenol diffusion mechanisms occur.

Therefore, either for phenol or ozone, a concentration gradient is assumed to exist from the periphery to the inside of the particle.

- The adsorption kinetics are affected by the operational conditions even during the process.

Redefining the terms of Eqs. 14 and 15, according to Eq. 11, through the term *z*, Eqs. 23 and 24 are obtained, which describe the variation of phenol concentration by oxidation in both the liquid phase and on the surface of the solid.

$$\left(-\frac{dC_P}{dt}\right)_{ox,L} = z\,k_{c,L}\,C_{O_3}\,C_P = k_{oxL}\,C_P \quad (23)$$

$$\left(-\frac{dC_P}{dt}\right)_{ox,s} = z\,k_{c,S}\,Z_{O_3}\,Z_P w^2 = k_{oxS} Z_P w \quad (24)$$

As can be show, the above equations contains, k_{oxL} and k_{oxS} constants, the factor *z*, the elemental kinetic constants $k_{c,L}$ and $k_{c,S}$, and the ozone concentrations C_{O3} and Z_{O3}. These ozone concentrations can be assumed constant after the initial transitory period.[40] If the diffusional L-S resistances are negligible, the ozone concentration in the solid is in equilibrium with that of the liquid, according to Eq. 19, to obtain:

$$C^*_{O_3} = m\,Z_{O_3} \approx C_{O_3} \quad (25)$$

The phenol concentration in the activated carbon, Z_P, depends on the adsorption process rate. In quick adsorption processes, Z_P is assumed to be in equilibrium with the phenol concentration in the liquid, C_P and is estimated from the Freundlich equation:[41]

$$Z_P = Z_{P,\infty} = K_F\left(C_P\right)^{\frac{1}{n_F}} \quad (26)$$

where C_P is the phenol concentration in the liquid, in equilibrium with Z_P, or phenol adsorbed in the active carbon particle. The constant K_F indicates the AC adsorption capacity, and n_F is the heterogeneity factor. However, the phenol concentration in the solid, Z_P, usually depends on the adsorption kinetics of the process and does not reach equilibrium during the process. On the other hand, the AC adsorption kinetics with ozone change significantly compared to the adsorption process without it.[42] This will be demonstrated later in this work with the estimated reaction and adsorption kinetic constants.

To describe the phenol adsorption kinetics dependence on AC, a pseudo-second order model is chosen, which has been conveniently verified in previous works,[42] according to:

$$\left(-\frac{dC_P}{dt}\right)_{ads} = \left(-\frac{dZ_P}{dt}\right)_{ads} w = k_{ads}\left(Z_{P,\infty} - Z_P\right)^2 w \quad (27)$$

where k_{ads} (g mg^{-1} min^{-1}) is the pseudo-second order kinetic constant. From Eqs. 23, 24 and 27, Eq. 28 is deduced to express the phenol removal in the Ad/Ox process.

$$-\frac{dC_P}{dt} = k_{oxL} C_P + k_{oxS}\,Z_P\,w + k_{ads}\left(Z_{P,\infty} - Z_P\right)^2 w \quad (28)$$

The adsorption phenomenon that occurs together with ozonisation may be quite different from that observed in its absence, so parameters k_{ads} and $Z_{P,\infty}$ should not be confused with those observed in Eqs. 33 and 38.

4. Results and discussion

4.1. Nitrogen adsorption studies

Fig. 3 shows the adsorption-desorption isotherms of Kemisorb® 530 GAC and PAC. According to the shape of the curves of Fig. 3a, an isotherm Type I is observed, in which at low relative pressures the amount of adsorbed nitrogen increases with the relative pressure due to the high interaction between active carbon and nitrogen, but without reaching any plateau, i.e., the solid does not clearly present the limit of its adsorption capacity. This is probably because thermodynamic equilibrium is not reached due to incomplete monolayer formation.[43]

Moreover, a hysteresis cycle was observed, which reveals a capillary condensation effect on the pores of the activated carbons, associated with the mesoporous part of the solid.

The physical properties of the activated carbons used in this work are shown in Table 2. GAC Kemisorb® 530 presents a BET surface area of 961.5 m^2 g^{-1} greater than that of PAC, which is 832.3 m^2 g^{-1}. However, PAC has a higher mesopore volume (V_M=0.20 cm^3 g^{-1}) and average pore diameter (35.0 Å), and should have greater adsorption capacity than the GAC Kemisorb® 530 for higher molecular weight compound removal. The micropore volume value of PAC corresponds to the macroporous region.[44]

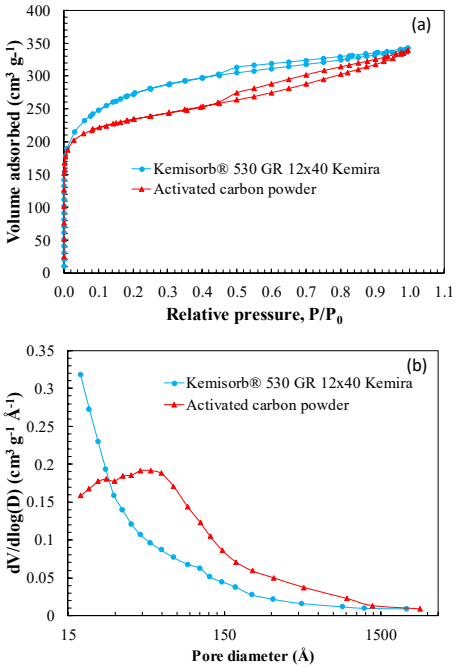

Fig. 3 Nitrogen adsorption-desorption isotherms and pore size distribution of Kemisorb® 530 GAC and powder activated carbon calculated using the BJH model.

Table 2 Surface properties of the activated carbons studied.

Property	Kemisorb® 530 GR 12x40 Kemira	Activated carbon powder
S_{BET}, $m^2\ g^{-1}$	961.5	832.3
S_{ext}, $m^2\ g^{-1}$	410.4	264.0
V_T, $cm^3\ g^{-1}$	0.38	0.44
V_μ, $cm^3\ g^{-1}$	0.24	0.24
V_M, $cm^3\ g^{-1}$	0.14	0.20
V_M/V_T, %	36.8	45.5
V_μ/V_T, %	63.2	54.5
D_P, Å	27.9	35.0

S_{BET} – BET surface area; S_{ext} – external surface area; V_T – total pore volume; V_μ - micropore volume; V_M – mesopore volume; V_M/V_T – mesopore percentage; V_μ/V_T – micropore percentage; D_P – average pore diameter.

4.2. Point-zero charge determination

During the phenol adsorption processes, the AC characteristics, such as molecular size, solubility, pK_a and adsorbate nature (i.e., aromatic or not) influence the adsorption process. As indicated in the previous section, molecular size controls the contaminant accessibility to the AC pores together with solubility, a consequence of hydrophobic interactions. These are greatly conditioned by the contaminant pK_a, and closely linked to the solution pH, as explained below.

Thus, the efficiency of the activated carbon in the Ad/Ox process can be affected by its point of zero charge (PZC). A surface charge is at its point of zero charge when the surface charge density equals zero. It is a negative logarithmic value for the activity of the charge-determining ions in the bulk phase.[45] According to Ferreiro et al.,[28] when the surface of the catalyst is positively charged, it favours interactions with anionic pollutants (pH < pH_{pzc}), whereas a negatively charged surface promotes interactions with cationic pollutants, due to the ionization of oxygenated functional groups (pH > pH_{pzc}).[29]

The experimental curve obtained by Silva et al. describes the method for Kemisorb® 530 GAC and PAC, shown in Fig. 4.[34] The point of zero charge, pH_{pzc}, of Kemisorb® 530 GAC was 9.69, whereas PAC was 10.19. The pH_{pzc} values obtained are the same as the typical values of fresh activated carbon (between 8 and 10), obtained by authors such as Valdés & Zaror and Adam[35,46]. This high PZC value is beneficial, since an increase in the acidity of the AC surface results in a decrease in the amount of phenol adsorbed.[47]

The point of zero charge together with the speciation of phenol, dependent on the solution pH, may influence the adsorptive behaviour of the activated carbon in terms of adsorption capacity. The acid ionization equation of phenol is shown in Eq. 29:[48]

$$C_6H_5OH\ (aq) + H_2O\ (l) \leftrightarrow C_6H_5O^-\ (aq) + H_3O^+\ (aq)\ pK_a=9.95 \qquad (29)$$

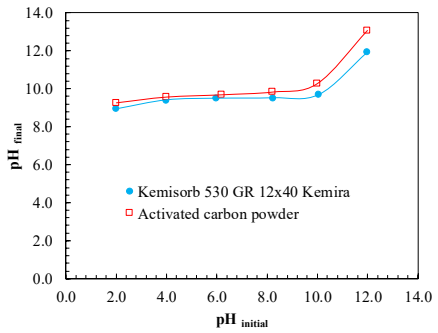

Fig. 4 Point of zero charge of Kemisorb® 530 and powder activated carbon determined by the acid-base titration method.

According to the pK_a value shown in Eq. 16, phenol is a very weak acid. For a pH lower than 9.95, the phenoxide ion concentration is negligible, while for a pH higher than 9.95, the phenol will be ionized and consequently the adsorption on the activated carbon will decrease due to electrostatic repulsion interactions. Thus, the overall reactivity of phenol towards ozone increases from 1300 $M^{-1}\ s^{-1}$ at pH < 9.9 to $1.4\times10^9\ M^{-1}\ s^{-1}$ at pH > 9.9.[49,50] Despite the favourable effect on ozonisation with alkaline pH, an industrial implementation would be unviable for the following reasons: i) chemical operating costs would increase by 36.1%,[51] ii) the adsorption stage would not be favoured, iii) pH adjustment would require more contact or residence time to adjust a wide range of pH, iv) it would be environmentally unsustainable, as the discharge pH must be between 6.0 and 8.0.[42]

4.3. Adsorption process of phenol onto AC and thermodynamic aspects

Adsorption isotherms are used to evaluate the adsorption capacity of active carbons for a specific pollutant. This tool enables discrimination between different active carbons, evaluating the adsorption phenomenon, in order to select the most suitable AC for a desired application.[47] To analyse the adsorption phenomenon in the two activated carbons under study, the equilibrium data obtained were adjusted to widely used models such as the Langmuir, Freundlich and Dubinin-Radushkevich Isotherm.[52] Fig. 5 shows the adsorption isotherms of phenol on Kemisorb® 530 and PAC at 15°C, 25°C and 35°C at pH=6.5.

As seen in Fig. 5a, PAC has an L-type isotherm without plateau according to the classification made by Limousin et al.[53] This type of isotherm indicates that the ratio between the amount of adsorbed phenol and the solution concentration decreases with the increased concentration in the equilibrium. Furthermore, this isotherm does not clearly present the limit of its adsorption capacity. However, the granular activated carbon Kemisorb® 530 shows a C-type isotherm (Fig. 5b), characteristic of materials in which the ratio q_e to C_e is almost constant at any concentration.

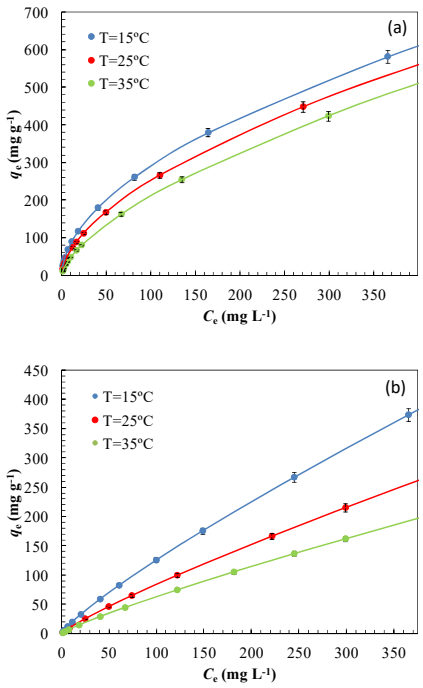

Fig. 5 Adsorption isotherms of phenol at pH=6.5 on two types of activated carbons at different temperatures fitted to the Freundlich isotherm model: (a) powder activated carbon and (b) Kemisorb® 530.

The mathematical representation of the three models mentioned is shown below. Dubinin-Radushkevich's Isotherm (D-R's model) is characteristic of single solute system,[35] and much more general than Langmuir's isotherm since it assumes the homogeneity of the surface according to:[54]

$$\ln q_\infty = \ln q_s - \beta\,\varepsilon^2 \tag{30}$$

where β is the activity coefficient related to the adsorption free energy E, expressed by:

$$E = \frac{1}{\sqrt{2\beta}} \tag{31}$$

and ε is the Polyani potential, expressed as a function of temperature through:[55]

$$\varepsilon = R\,T\,\ln\left(1+\frac{1}{C_\infty}\right) \tag{32}$$

The linearized Freundlich equation is given by:[56]

$$\ln q_\infty = \ln K_F + \frac{1}{n_F}\ln C_\infty, \tag{33}$$

in which n_F refers to the process irreversibility, so values clearly greater than one mean spontaneous adsorption.

Langmuir's model assumes the formation of a monolayer on the surface of activated carbon with minimal interaction among the adsorbate molecules (phenol), and the adsorption sites having the same adsorption energy. The linearized Langmuir equation is given by Enniya et al.:[57]

$$\frac{C_\infty}{q_\infty} = \frac{1}{q_{max}\,K_L} + \frac{1}{q_{max}}\,C_\infty \tag{34}$$

where K_L is the equilibrium constant related to the affinity of the binding sites and adsorption nature, and q_{max} is the monolayer adsorption capacity. According to Gupta et al.,[58] the tendency of phenol to be adsorbed onto the adsorbent surface, also related to the isotherm type, is described using the dimensionless parameter R_L:

$$R_L = \frac{1}{1+K_L\,C_0} \tag{35}$$

Based on R_L, a simple evaluation of the adsorption characteristics can be performed under the following conditions: i) when R_L>1, the process is unfavourable, ii) when R_L=1, the adsorption isotherm is linear, iii) when 0<R_L<1, the process is favourable, and iv) when R_L=0, the process is irreversible.

Table 3 shows the adjustment parameters obtained by the different adsorption models. Based on the regression analysis of the experimental data obtained from phenol adsorption, it may be inferred, with an adjustment coefficient of $R^2 \cong 0.98$, that the phenol adsorption on either PAC or GAC Kemisorb® 530 GR is fairly described with Freundlich's model for all studied temperatures. Moreover, n_F is greater than one for the two types of carbon used, proving a favourable adsorption process.[54]

According to D-R's model parameters shown in Table 3, the adsorption energy value is much higher for GAC Kemisorb® 530 than for powdered activated carbon, proving that adsorption on PAC is more favoured than on Kemisorb® 530.

Finally, as far as the parameters obtained from Langmuir's model are concerned, the maximum adsorption capacity of phenol, q_{max}, increases as the temperature decreases from 384.61 mg g^{-1} to 588.23 mg g^{-1}, on powdered activated carbon, and from 112.81 mg g^{-1} to 400.00 mg g^{-1} on GAC Kemisorb® 530, proving that adsorption on both carbons are exothermic. In addition, the low values of Langmuir's equilibrium constant suggest a weak interaction of phenol with the surface of the two types of carbons, as observed in Table 3. The separation factor obtained in both carbons indicates that the adsorption process is favourable, as predicted by Freundlich's model.

The maximum amounts of adsorbed phenol, q_{max}, of PAC and GAC are compared with others from the bibliography study by Ma et al.[59] The carbons selected for this work have q_{max} values of 588.23 mg g^{-1} for PAC and 400.00 mg g^{-1} for GAC Kemisorb® 530, against those of other materials such as ACs from bamboo (with 59.62 mg g^{-1}) or from coconut shell (with 45.45 mg g^{-1}). Nevertheless, the latter two have larger specific surface areas (over 1000 m^2 g^{-1} versus 900 m^2 g^{-1} for the carbons studied here). Moreover, the ACs referred to by Ma et al. have an average pore diameter lower than 27 Å, and consequently, the accessibility of molecules such as phenol is impeded because of their high microporosity.[59] Therefore, carbons with high microporosity (unlike the ones studied in this work),

present a greater diffusion resistance and are not suitable for phenol removal.

PAC and GAC adsorption were analysed following three different kinetic models: pseudo-first order, pseudo-second order and intraparticle diffusion. Fig. 6 shows the evolution of the adsorption kinetics of phenol onto PAC and GAC Kemisorb® 530 GR at 15°C, 25°C and 35°C, maintaining pH=6.5 in all cases.

The pseudo first-order kinetic model is given by Eq. 36, according to Markandeya et al.[41]

$$\frac{dq_t}{dt} = k_1 (q_\infty - q_t) \quad (36)$$

where k_1 is the pseudo-first-order rate constant. Integrating and linearizing Eq. 36 for the boundary conditions, q_t=0 at t=0, leads to the following expression:

$$\log (q_\infty - q_t) = \log q_\infty - \frac{k_1}{2.303} t \quad (37)$$

The pseudo-second-order model is represented as:[60]

$$\frac{dq_t}{dt} = k_2 (q_\infty - q_t)^2 \quad (38)$$

where k_2 is the pseudo-second-order rate constant. Integrating and rearranging Eq. 38 for the initial conditions, q_t=0 at t=0, the following equation is obtained:

$$\frac{t}{q_t} = \frac{1}{k_2 q_\infty^2} + \frac{1}{q_\infty} t \quad (39)$$

Finally, the intraparticle diffusion model is given by:[54]

$$q_t = k_{dif} \sqrt{t} + C_{id} \quad (40)$$

where k_{dif} is the intraparticle diffusion rate constant and C_{id} the amount of phenol adsorbed in a short period of time. The dimensionless factor R_i enables determining the initial adsorbed amount according to Ferreiro et al.[42]

$$R_i = 1 - \frac{C_{id}}{q_{max}} \quad (41)$$

Table 4 shows the fit parameters obtained for the three kinetic models proposed for 15, 25 and 35°C.

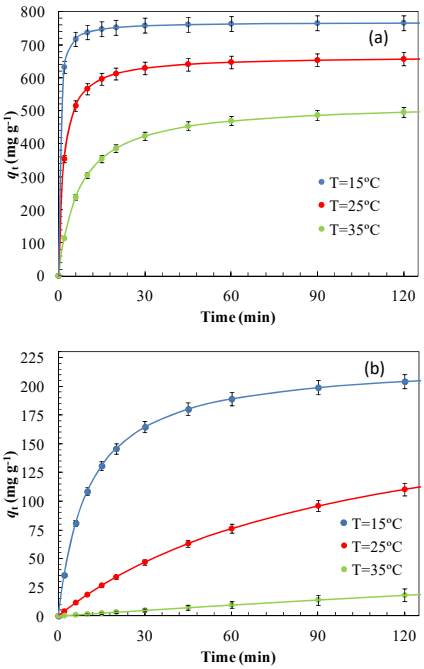

Fig. 6 Modelling of a pseudo-second-order kinetics of the adsorption process onto: (a) powdered activated carbon and (b) GAC Kemisorb® 530 GR.

Table 3 Adsorption isotherm parameters for phenol adsorption onto activated carbon powder and Kemisorb® 530 at different temperatures.

Adsorbent	**Activated carbon powder**			**Kemisorb® 530 GR 12x40 Kemira**		
Isotherm Model	Temperature, °C			Temperature, °C		
	15	25	35	15	25	35
Langmuir						
K_L, L mg^{-1}	0.122	0.016	0.0062	0.029	0.007	0.001
q_{max}, mg g^{-1}	588.23	400.00	384.61	400.00	256.41	112.81
R^2	0.889	0.882	0.896	0.845	0.893	0.877
R_L values	0.008	0.058	0.296	0.033	0.125	0.350
Freundlich						
K_F, (mg g^{-1}) (L mg^{-1})$^{1/n}$	25.10	17.60	11.26	2.63	1.64	1.18
n_F	1.87	1.73	1.57	1.19	1.16	1.15
R^2	0.997	0.998	0.983	0.988	0.984	0.990
Dubinin-Radushkevich						
q_s, mg g^{-1}	426.62	411.37	380.16	252.67	152.14	105.49
β, mol^2 kJ^{-2}	196.35	317.66	357.99	169.02	233.12	419.71
E, kJ mol^{-1}	0.050	0.040	0.037	0.054	0.046	0.035

R^2	0.754	0.787	0.859	0.924	0.967	0.951

Table 4 Kinetic parameters for the adsorption of phenol onto activated carbon powder and Kemisorb® 530 at different temperatures.

Adsorbent	**Powder Activated Carbon**			**Kemisorb® 530 GR 12x40 Kemira**		
Kinetic Model	Temperature, °C			Temperature, °C		
	15	25	35	15	25	35
Pseudo-1st order						
k_1, min^{-1}	0.0169	0.0085	0.0011	0.0019	0.0013	0.0002
R^2	0.984	0.992	0.914	0.826	0.783	0.707
Pseudo-2nd order						
k_2, g mg^{-1} min^{-1}	3.01×10^{-3}	8.52×10^{-4}	2.62×10^{-4}	4.29×10^{-4}	5.12×10^{-5}	7.01×10^{-6}
R^2	0.997	0.997	0.992	0.991	0.995	0.997
Intraparticle diffusion						
k_{dif}, mg g^{-1} $min^{-0.5}$	60.57	48.08	30.05	28.58	9.76	1.10
C_{id}, mg g^{-1}	3.65	72.02	81.05	7.37	8.01	11.13
R^2	0.669	0.753	0.908	0.933	0.950	0.787
R_i	0.99	0.82	0.79	0.98	0.97	0.90

The regression analysis of experimental data obtained from phenol adsorption shows a determination coefficient $R^2 \cong 0.99$, indicating that the pseudo-second-order model is best at describing the phenol adsorption kinetics either for PAC or GAC Kemisorb® 530. According to Ho and McKay,[60] adsorption cases following the second-order model proves a chemical-step controlled adsorption process. The mechanism of the adsorption phenomenon that takes place consists of the following stages:[42] (i) external mass transfer from the aqueous medium to the boundary film, (ii) mass transfer from the boundary film to the activated carbon external surface, (iii) mass transfer in the pores, (iv) adsorption onto activated carbon active sites (intermediately initial adsorption at low temperatures according with obtained R_i values), and v) internal diffusion.

Parameter C_{id} in the intra-particle diffusion model indicates that the adsorption of phenol can take place in multiple steps. Consequently, the intra-particle diffusion is not the only rate limiting step.

The above results were confirmed by the evaluation of thermodynamic parameters. Enthalpy, entropy and free energy changes in the adsorption mechanism were determined through the following expressions:[56]

$$\Delta G^\circ = -RT\ln K_L \qquad (42)$$

where ΔG° is the standard Gibbs free energy, R is the universal gas constant, T is the absolute temperature and K_L is the equilibrium constant. Enthalpy and entropy values were determined through the Van't Hoff equation:[54,57]

$$\ln K_L = \frac{\Delta S^\circ}{R} - \frac{\Delta H^\circ}{R}\frac{1}{T} \qquad (43)$$

where ΔS° is the entropy change and ΔH° is the enthalpy change associated with the adsorption process. The thermodynamic parameters of the phenol adsorption onto both ACs are given in Table 5.

Table 5 shows the negative enthalpy values determined for GAC Kemisorb® 530 and PAC, characteristic of an exothermic process. According to Adam,[35] enthalpy changes in the range 0-84 kJ mol^{-1} indicate a physisorption mechanism, while values between 84 and 420 kJ mol^{-1} are typical of chemisorption mechanisms. The entropy change (287.082 J mol^{-1} K^{-1} for Kemisorb® 530 and 427.748 J mol^{-1} K^{-1} for PAC) reflects the randomness increase between the solution and solid interface and, consequently, structural changes in the activated carbons and phenol.[42,57]

The negative free energy change values indicate feasibility and the spontaneous nature of phenol adsorption on both activated carbons. The observed free energy increment. From -18.959 to -13.217 kJ mol^{-1} for the GAC Kemisorb® 530, and from -22.415 to -13.860 kJ mol^{-1} for the PAC, when temperature increases from 15 to 35°C, proves better adsorption occurs at low temperatures.

Table 5 Thermodynamic parameters of phenol adsorption onto both ACs.

Adsorbent	***T*, °C**	***K*L, L mol^{-1}**	**Δ*H*, kJ mol^{-1}**	**Δ*S*, J mol^{-1} K^{-1}**	**Δ*G*, kJ mol^{-1}**	***Ea*, kJ mol^{-1}**	***k0***
Kemisorb® 530	15	2735.06			-18.959		
	25	658.77	-101.679	287.082	-16.088	151.9	1.24×10^{-31}
	35	174.03			-13.217		
PAC	15	11573.66	-145.671	427.748	-22.415	90.15	1.36×10^{-19}

	25	1505.76		-18.137
	35	223.63		-13.860

In addition, the activation energy was estimated from kinetic data taken at 15, 25 and 35°C. The activation energy value was estimated through the Arrhenius equation:[61]

$$\ln k_2 = \ln k_0 - \frac{E_a}{R}\frac{1}{T}, \quad (44)$$

where k_0 is the frequency factor and E_a is the activation energy for the adsorption process. According to Ferreiro et al. and Fil et al.,[42,62] E_a values are a consequence of the type of adsorption phenomena. Values between 88 and 400 kJ mol^{-1} correspond to a chemical adsorption. Thus, values of 151.9 kJ mol^{-1} for GAC Kemisorb® 530, and 90.15 kJ mol^{-1} for PAC, correspond to chemisorption mechanisms.

4.4. Activated carbon activity comparison

This section discusses the results simultaneously obtained in an Ad/Ox process using a bed of activated carbon packed in a cartridge in the reactor, as seen in Fig. 1, compared with those from simple ozonation.

The operational conditions employed in the batch experiments were: Q_G=4.0 L/min, $C_{O_3,G}$=19.0 mg/L, C_0=1000.0 mg/L, pH=6.5 and M=500.0 g. First, the results obtained through a simple ozonation process were compared, and those obtained through an Ad/Ox process were analysed and are shown in Fig. 7.

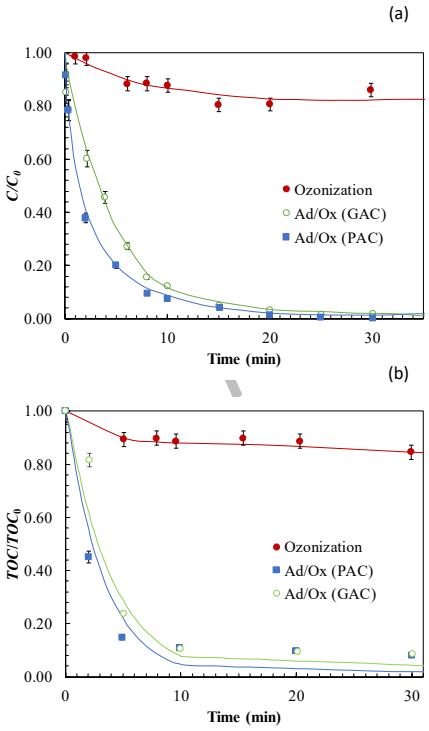

Fig. 7 Comparison of the degradation of phenol (a) and mineralisation (b) with ozonisation and Ad/Ox processes. Experimental conditions: C_0=1000.0 mg L^{-1}, Q_G=4.0 L min^{-1}, $C_{O_3,G}$=19.0 mg L^{-1}, pH=6.5, V=10.0 L, T=20°C, m_{GAC}=500.0 g.

The phenol removal improvement with the Ad/Ox process is evident, since a 100% removal efficiency was achieved. The simultaneous combination of ozonation and adsorption processes, both with CAP and GAC, causes a significant increase both in primary degradation kinetics and the mineralization degree compared to simple ozonation.

Fig. 7 shows the phenol removal results of 100% removal in just 30 minutes for a 1000 mg/L phenol concentration. Additionally, mineralization exceeding 80% was achieved (not shown in Fig. 7). Therefore, the results indicate that the use of GAC in Ad/Ox processes cause superior results in phenol removal and mineralization, despite using a lower dose of ozone. The type of activated carbon (GAC or PAC) does not seem to influence the oxidation efficiency. The generation of radicals on the AC surface explains the higher speed of reaction in the liquid.[13,33]

After the analysis of the first results about simple ozonation and the different types of sequential Ad/Ox processes, the appropriateness of the simultaneous Ad/Ox process with both GAC and PAC was postulated. Ad/Ox with GAC was selected for the remainder of the experiments because of the handling advantages of the granulated material. In addition, GAC Kemisorb® 530 is extensively used in water potabilization facilities due to, among other factors, its low cost, easy reuse and regeneration, and treatment unit, making it the most suitable type of activated carbon for fixed bed contact systems.[63] PAC is generally used in treatment plants with mixing units for coagulation purposes, where PAC is suspended in the water to be treated.[64]

4.5. Kinetic analysis of the Ad/Ox process

Ad/Ox ozonation experiments were performed under the ozone flow and concentration conditions indicated in the 'Experimental methods' section. The process was applied in all cases to a 1000.0 mg L^{-1} phenol solution, varying the amount of GAC in the cartridge, using a mass of 250.0 g or 500.0 g according to the experiment.

The phenol degradation results for both primary degradation and mineralization were obtained by measuring the total organic carbon (TOC) in the treated solution. The degradation kinetics were adjusted to the proposed model in Section 3, by solving Eqs. 18 and 20. The solution process for these equations involved the FlexPDE® calculation tool, a simulation programme used here to determine, through a corresponding fitting process, the kinetic constants of adsorption and ozonation and the modelled kinetics of phenol concentration and TOC during degradation. Because the fluid velocity is large enough to be operating in a turbulent regime, it was assumed that the GAC load confined inside the cartridge (see Fig. 1), behaves as if it was perfectly distributed in the reactor, due to the vigorous agitation of the reaction medium through the recirculation system. Consequently, the kinetic

parameters of oxidation in the liquid and solid and adsorption phenomena will be affected by the mixing conditions in the ozonator through G-L and L-S flows and the corresponding mass transfer parameters.

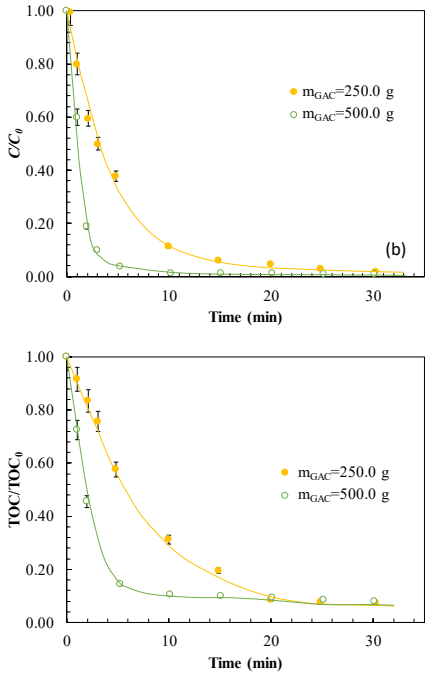

Fig 8. Experimental and modelled kinetic profiles of phenol degradation in an Ad/Ox process for phenol degradation, varying the amount of GAC in the cartridge: (a) Primary degradation of phenol and (b) Evolution of mineralisation. Experimental conditions: C_0=1000.0 mg L^{-1}, Q_G =4.0 L min^{-1}, $C_{O_3,G}$=19.0 mg L^{-1}, pH=6.5, V=10.0 L, T=20°C.

The initial conditions or value of the dependent variables involved in the differential equations at time zero (the starting time for the Ad/Ox phenol removal process) were defined before the calculus process. The concentration at any position within the reactor is C_P=C_0=1000.0 mg L^{-1} and therefore the load placed on the bed of activated carbon is zero, Z_P=0.0 mg g^{-1}. The programme simulates the degradation kinetics on the basis of the value of the initial variables, varying parameters to calculate k_{ads}, k_{oxL} and k_{oxS} to achieve the best fit to the experimental degradation kinetics.

Kinetics modelling of the experimental degradation was carried out for two different amounts of GAC, 250.0 and 500.0 g. In Fig. 8, fittings of the experimental data are shown to the kinetic model proposed for the two different GAC quantities loaded in the reaction media. Fig. 8 shows that an increase in catalyst dosage provides more active surface sites, thus facilitating decomposition of ozone molecules into more hydroxyl radicals.[65] The previously mentioned kinetic model was also employed in the analysis of mineralization. The TOC values were used in this case as the experimental results. Similar to the primary degradation, the TOC results were fitted to the proposed model; the results are shown in Fig. 8. The fitting result was good, yielding a determination coefficient R^2=0.95 for primary degradation fitting and R^2=0.99 for mineralisation fitting. Similarly, Table 6 also shows the values of the obtained adsorption and oxidation kinetic constants to fit the experimental kinetics for a simultaneous Ad/Ox process.

Table 6 shows the constants obtained in the fitting process, which reveal that an increased GAC amount does not affect the constant of oxidation in the solid (which is similar in both cases), but contributes to an increased oxidation constant k_{oxL} in the liquid. This apparent constant includes the ozone concentration in the liquid and a coefficient z that depends strongly on the efficiency and concentration of $OH^{\bullet}$ (see Eq. 15), clearly influenced by the catalytic activity of the GAC surface that competes with the adsorptive capacity. An equilibrium balance in GAC's dual role (adsorbent-reactive) is essential to develop good Ad/OX process efficiency.[66]

Conversely, the value of the oxidation constant in the liquid, k_{oxL}, is halved in mineralization compared to the primary degradation value, because of the more refractory nature of degradation intermediates.[67] Another effect observed in k_{oxL} is a continuous decline as the process goes on, as a result of the progressive occupation of the GAC surface by the phenol and its derivatives.

4.6. Analysis of successive Ad/Ox cycles and regeneration

In view of the good results obtained with an Ad/Ox simultaneous process, the possibility of several consecutive cycles was assessed to see the extent of the changes in the GAC's adsorptive properties. It is interesting to quantify the number of consecutive cycles that can be performed using the same fixed bed of GAC, until it completely loses its adsorption capacity or deactivates. Initially, we performed two consecutive Ad/Ox cycles of 30 minutes each, with the same operational conditions as discussed above.

Table 6 Summary of the kinetic constants of adsorption and oxidation related to the removal of phenol and mineralisation for 1 Ad/Ox cycle. Experimental conditions: C_0=1000.0 mg L^{-1}, Q_G =4.0 L min^{-1}, $C_{O_3,G}$=19.0 mg L^{-1}, pH=6.5, V=10.0 L, T=20°C.

Evolution	Kinetic parameter (a)	GAC CATALYST LOADING, g	
		250	500
Phenol removal	$k_{ads} \times 10^5$, min^{-1}	4.0	9.0
	$k_{oxL} \times 10^1$, min^{-1}	2.5/1.0	7.0/1.0
	$k_{oxS} \times 10^1$, $(mg\ L^{-1}) / (mg\ min\ g^{-1})$	0.1	0.1
Mineralisation	$k_{ads} \times 10^5$, min^{-1}	4.0	9.0
	$k_{oxL} \times 10^1$, min^{-1}	1.4/0.9	3.0/0.1
	$k_{oxS} \times 10^1$, $(mg\ L^{-1}) / (mg\ min\ g^{-1})$	0.1	0.1

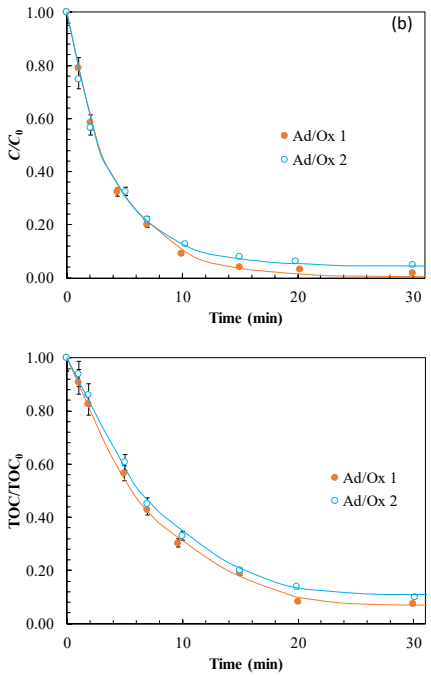

Fig. 9 Comparison of removal efficiencies in Ad/Ox consecutive cycles: (a) primary degradation of phenol and (b) mineralization or TOC removal. Experimental conditions: C_0=1000.0 mg L^{-1}, Q_G =4.0 L min^{-1}, $C_{O_3,G}$=19.0 mg L^{-1}, pH=6.5, V=10.0 L, T=20°C, m_{GAC}=250.0 g.

The same experimental conditions of the previous section were used, but with only 250.0 g of GAC for the consecutive cycle's experiments. The reactor was fed with 10 L of 1000.0 mg L^{-1} phenol solution, covering 30 minutes of process to complete the first cycle (Ad/Ox 1). The solution was then extracted and a new 1000.0 mg L^{-1} phenol solution was introduced, while keeping the previously loaded GAC.

According to Fig. 9, the fitting results were good, yielding a determination coefficient R^2=0.98 for primary degradation fitting and R^2=0.99 for mineralization fitting. Fig. 9 shows the results obtained for the primary degradation and for mineralization in cycles 1 and 2 are similar, above 95% in the first cycle and 80% in the second cycle. This result may have two possible causes. The first is the amount of GAC in the cartridge is large with respect to the phenol solution and does not reach saturation in the first cycle; there are active centres free to continue with the dissolution of phenol adsorption.[25] The second effect is that ozone acts directly on the bed of GAC, cleaning active centres and allowing an additional quantity of phenol to be adsorbed.[32] In any case, the adsorption is altered by oxidation at the surface of the granular activated carbon.

After an analysis of the behaviour of two consecutive cycles to discover the advantages and disadvantages of a combined process compared with a simple process, the consecutive Ad/Ox cycles with same activated carbon were analysed. The kinetic constants were also determined following the previously mentioned procedure for an Ad/Ox cycle, taking into account that the GAC in the cartridge was not changed from one cycle to another. Then, when an additional cycle starts, the amount of phenol adsorbed on the AC is nonzero; it was necessary to define a starting Z_P value, different and growing as the number of cycles increases. Thus, the Z_P to initiate the calculus process of the FlexPDE® software for the beginning of the second cycle is the final Z_P of the first cycle, and the value at the beginning of the third cycle will be the value at the end of the second cycle, and so on.

The adsorption and oxidation kinetic constants obtained for 6 consecutive Ad/Ox cycles with 250.0 and 500.0 g GAC amounts are presented in Tables 7 and 8, respectively.

In view of the results in Table 7, the oxidation occurs predominantly in the liquid since the kinetic constants in the liquid are considerably higher than in the solid. This finding could be due to the contribution of the GAC in reactions, only as free radical generators, that involved are in the oxidation in the bulk liquid. However, the value of these constants decreases when the number of cycles increases, which can be explained by the decreasing of free active centres, since the GAC deteriorates or becomes covered by phenol and other compounds by oxidation.[29,42]

The kinetic adsorption constant on the solid surface, k_{ads} and the corresponding oxidation constant k_{oxS}, are fairly constant as the number of consecutive Ad/Ox cycles increases, since not enough phenol or intermediate compounds has been adsorbed to modify the surface of the activated carbon.[68] On the other hand, neither constant appears to be modified during mineralization. Accordingly, the reagent mechanisms on the GAC surface seem to be more significant for mineralization.[69]

Table 7 Summary of the adsorption and oxidation kinetic constants for the primary degradation of phenol solution and mineralisation, for 6 cycles with m_{GAC}=250.0 g. Experimental conditions: C_0=1000.0 mg L^{-1}, Q_G =4.0 L min^{-1}, $C_{O_3,G}$=19.0 mg L^{-1}, pH=6.5, V=10.0 L, T=20°C.

Evolution	Kinetic parameter	Cycle nº					
		1	2	3	4	5	6
Phenol removal	$k_{ads} \times 10^5$, min^{-1}	4.0	4.0	4.0	4.0	4.0	4.0
	$k_{oxL} \times 10^1$, min^{-1}	2.5/1.0	2.2/1.0	1.6/0.8	1.1/0.6	1.0/0.4	0.8/0.2
	$k_{oxS} \times 10^1$, (mg L^{-1}) / (mg min g^{-1})	0.1	0.1	0.1	0.1	0.1	0.1
Mineralisation	$k_{ads} \times 10^5$, min^{-1}	4.0	4.0	4.0	4.0	4.0	4.0
	$k_{oxL} \times 10^1$, min^{-1}	1.4/0.9	1.2/0.9	1.0/0.9	0.6/0.5	0.6/0.3	0.4/0.3
	$k_{oxS} \times 10^1$, (mg L^{-1}) / (mg min g^{-1})	0.1	0.1	0.1	0.1	0.1	0.1

Table 8 Summary of adsorption and oxidation kinetic constants up to 6 cycles during oxidation of phenol solutions. Experimental conditions: C_0=1000.0 mg L^{-1}, Q_G =4.0 L min^{-1}, $C_{O_3,G}$=19.0 mg L^{-1}, pH=6.5, V=10.0 L, T=20°C, m_{GAC}=500.0 g.

Evolution	Kinetic parameter	Cycle nº					
		1	2	3	4	5	6
Phenol removal	$k_{ads} \times 10^5$, min^{-1}	9.0	9.0	7.0/3.0	1.0	1.0	1.0
	$k_{oxL} \times 10^1$, min^{-1}	7.0/1.0	3.0/1.0	3.0/1.0	2.0/1.0	2.0/0.5	2.0/0.5
	$k_{oxS} \times 10^1$, (mg L^{-1}) / (mg min g^{-1})	0.1	0.1	0.1	0.1	0.1	0.1
Mineralisation	$k_{ads} \times 10^5$, min^{-1}	9.0	9.0	7.0	1.0	1.0	1.0
	$k_{oxL} \times 10^1$, min^{-1}	3.0/0.1	2.5/0.1	2.0/0.1	1.8/0.1	1.6/0.1	1.4/0.1
	$k_{oxS} \times 10^1$, (mg L^{-1}) / (mg min g^{-1})	0.1	0.1	0.1	0.1	0.1	0.1

Using a fixed bed of 500.0 g of GAC, a considerable increase in the oxidation kinetic constant in the liquid was observed, nearly 100 times the kinetic constant of oxidation in liquid in a non-catalytic ozonisation process, which is 0.09 min^{-1}, under the same operational conditions. This can be explained by a competition between the ozone and phenol flows at the GAC surface.[70] The dominance of the phenol flow involves the formation of layers of phenol on the GAC; the adsorption of this phenol will result in the deactivation of the GAC active centres and a decrease in its adsorptive and reactive capacities.[71,72] Otherwise, it would lead to an excess of radicalary activity, causing ineffective decomposition of ozone.[13]

The analysis of kinetic constants obtained for 250.0 and 500.0 g GAC shows that phenol oxidation is produced mostly in the liquid, although it should be noted that all of the constants shown in Table 7 and Table 8 decrease as the number of cycles increases.

In the case of the adsorption kinetics, despite adsorption constants having the same order of magnitude, they also decrease when the number of cycles increases.[68] The only constant that holds a value independent of the number of cycles is k_{oxS}. Consequently, constant k_{oxL} includes both the oxidation occurring in the liquid and that as a result of the generation of radicals in the solid surface, and reflects most of the oxidative activity of the system as a whole. This constant decreases as the number of cycles increases; this relationship is a direct consequence of GAC deterioration. Thus, GAC active centres experience a continuous decrease in their catalyst activity and consequently a progressive decrease in radical generation.[66]

Following the same procedure, mineralization was analysed and the corresponding constants were determined, using the same kinetic model as the primary degradation but replacing the phenol concentration with TOC values.

From Table 8, in the mineralization, as in the primary degradation, most secondary compounds oxidize in the liquid. The presence of GAC triggers a high quantity of radicals that cause a considerable increase the kinetic oxidation constant in the first cycles, when the active sites are free.[73] Nevertheless, the k_{oxL} values related to mineralisation in this case are lower, since the secondary compounds formed in the reaction are much more refractory.[74] Remarkably, in the case of 250.0 g of GAC, both constant adsorption kinetics and the oxidation constant in the solid are constant and independent of the number of cycles. This behaviour is explained because the GAC reaches the complete development of its activity.[47]

The increase in kinetic oxidation constant in the liquid was double that of the kinetic oxidation constant in liquid in a non-catalytic ozonisation process, estimated at 0.15 min^{-1}, while using a bed of 500.0 g of GAC, due to the greater radical activity of a GAC surface less occupied by adsorbed phenol. When

comparing the kinetic constants obtained in the primary degradation with those of mineralization, for this last case, the constants are lower in all cases by the amount of intermediate products such as acetic acid,[18] increasingly refractory, as the reaction progresses.

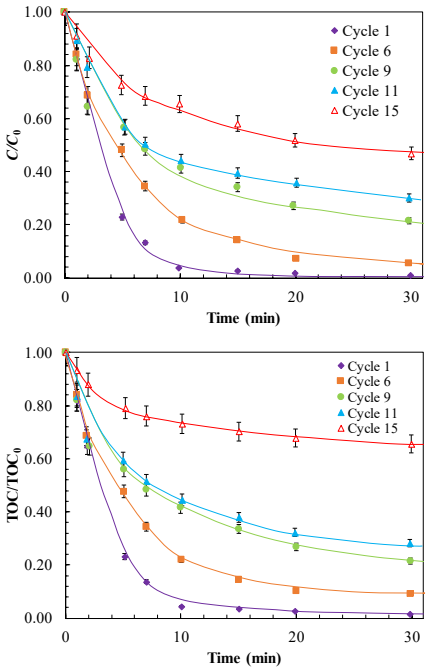

Fig. 10 Effect of the successive number of use cycles on an Ad/Ox process. (a) Phenol removal and (b) Mineralisation. Experimental conditions: C_0=1000.0 mg L^{-1}, Q_G =4.0 L min^{-1}, $C_{O_3,\,G}$=19.0 mg L^{-1}, pH=6.5, V=10.0 L, T=20°C, m_{GAC}=500.0 g.

A series of experiments of 9, 12 and 15 Ad/Ox cycles was performed, in which the phenol removal and the mineralization degree was observed and measured as the number of cycles increases (see Fig. 10). According to Fig. 10, the fitting results were good, presenting a determination coefficient R^2=0.97 for primary degradation fitting and R^2=0.99 for mineralization fitting. Oxidation kinetics were slower as the GAC deteriorates to cycle number 15. The results seem to indicate that if the number of cycles continues to rise, the kinetics could approach the behaviour of non-catalytic ozonation. Consequently, the activated carbon would not have any reactive and catalytic activity, leading to a less efficient use of ozone.[75,76]

Fig. 10 shows the progress of successive Ad/Ox 30 min cycles, which cause a gradual decrement in the phenol removal from the solution; i.e., 100% phenol is eliminated in the first cycle, while in cycle number 9, it decreases to 70%, and after 15 cycles, Ad/Ox barely removes 40% of the initial phenol.

In addition to the phenol removal, the effect of increasing cycle number on mineralization was analysed. The mineralization degree is very similar to the primary degradation in the early cycles. The GAC characteristics do not change the very significant participation of the activated carbon surface in the degree of mineralization; it is about the same order as the early cycles (until cycle 9; see Fig. 10). Only when the number of cycles is high (>9) primary degradation is more intense than the mineralization as a result of a remarkable loss of GAC reactivity. Decreasing GAC reactivity significantly influences the mineralization and to a lesser extent the primary degradation, which is less dependent on the surface of the activated carbon.[77]

Clearly, when the number of cycles increases, the Ad/Ox process tends to approach that of non-catalytic ozonation, either for primary degradation of phenol or for mineralization, which means that the GAC will deteriorate, losing efficiency and activity in the phenol degradation reaction system.

The surface area of the activated carbon is often coated by the adsorbate. Thus, when the GAC catalytic bed reaches the maximum phenol adsorption capacity, it must be regenerated to remove the phenol before reuse. In many occasions, the cost of the complete replacement of a fixed bed of GAC by another with pristine GAC is prohibitive.[36] The economics of a regeneration method could be a deciding factor when choosing the appropriate adsorbent for a given application.[78]

Therefore, in order to design a more sustainable process, two chemical regeneration techniques were studied, regeneration with NaOH and with ozone. Among the advantages of a regenerative Ad/Ox processes over an Ad/Ox with AC replacement are the process robustness, waste reduction and a cost savings of up to 50%. The cost of replacing a virgin GAC is approximately between $0.70-$1.20/lb while the cost of regeneration ranges between $0.50-$0.78/lb. The operating costs of this operation depend on the wastewater effluent characteristics and the GAC adsorption capacity.[79]

Fig. 11 compares the results of either phenol removal or mineralization degree, under the conditions described in this section for two Ad-Ox cycles with intermediate regeneration stages.

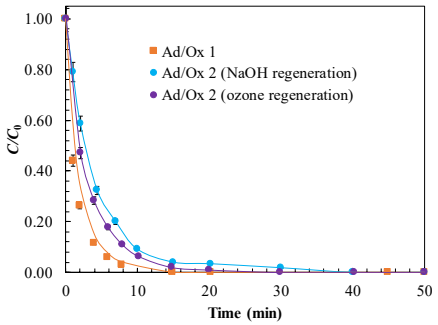

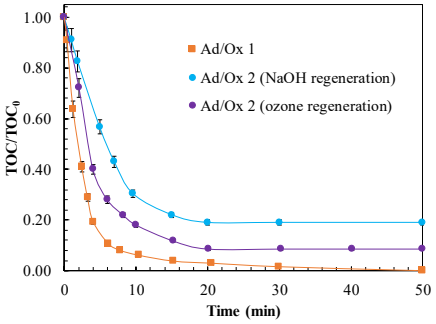

Fig. 11 Degradation kinetics of the phenol: (a) primary and (b) mineralization, using the NaOH and ozone regeneration methods for GAC Chemisorb® 530. Experimental conditions: C_0=1000.0 mg L^{-1}, Q_G =4.0 L min^{-1}, $C_{O_3,G}$=19.0 mg L^{-1}, pH=6.5, V=10.0 L, T=20°C, m_{GAC}=500.0 g.

Even though NaOH regeneration is a widely used treatment,[36,37] the post-regeneration mineralization obtained with this method was poor, losing 20% of the mineralizing capacity observed in the first cycle. This treatment is based on the modification of the surface polarity of the oxides in the carbon, since alkaline pH reduces the sorption forces. In addition, NaOH can promote decomposition or hydrolysis of phenol, reducing its sorption over GAC.[80] From the results shown in Fig. 11, this regeneration strategy it does not appear to be suitable for recovering the initial properties of GAC.

Conversely, regeneration with ozone resulted in a greater catalytic activity recovery, reaching a regeneration percentage of 91.5% degradation of phenol and phenol by-products. According to Álvarez et al. and Vega & Valdes,[39,77] this result may be because the O_3/GAC ratio used during the regeneration stage leads to a lower formation of acidic oxygen groups on the surface (SOG), which are responsible for creating obstructions in the entrance of micropores, which may inhibit the adsorption of phenol during use after the regeneration stage.

Conclusions

The combination of adsorption and ozonation (an Ad/Ox process), simultaneously with PAC or GAC, produces an improvement in both the kinetics of phenol removal and the mineralization degree compared to a simple ozonation process, even using low ozone dosages. The elimination improvement less related to the AC adsorptive capacity than to the generation of radicals that operate mainly in the liquid.

GAC has a favourable effect, obtained through an Ad/Ox process, compared with a simple ozonation process. The improvement in the amount of phenol eliminated is evident with values exceeding 100% in all analysed cases. The kinetic constants of adsorption, k_{ads}, is a fundamental parameter to characterize the batch adsorption-ozonation process. This, together with Freundlich adsorption parameters, is fundamental for adjusting the experimental data during the initial transient period. An appropriate combination of both, together with the ozonation kinetics concerning k_{oxL} in the liquid and k_{oxS} in the solid determine not only the initial transient stage but also the time to reach a steady state.

The succession of consecutive cycles does not affect the oxidation constant observed in the solid, k_{oxS}, either for mineralization or for primary degradation, suggesting the decisive participation of surface phenomena on mineralization. In contrast, the value of the oxidation constant in the liquid, k_{oxL}, becomes halved during mineralization compared with phenol removal, because of the more refractory nature of degradation intermediates. Another observed effect involves the continuous decrease of k_{oxL} as a consequence of the progressive occupation of the GAC surface by the phenol and its derivatives during the process.

During simultaneous Ad/Ox, the predominant ozone action occurs in the liquid phase because of the greater oxidation constants than in the solid. The value of these liquid phase kinetic oxidation constants decreases as the number of cycles increases, likely due to the decrease in active centres in the GAC, causing the generation of radicals to decrease. Consequently, as the number of cycles increases, the removal efficiency approaches that obtained through simple ozonation, both for primary mineralization and phenol elimination, which indicates that the GAC has deteriorating adsorptive and reactive functions.

Nomenclature

a_1	specific contact area G-L, m^{-1}
a_2	specific contact area L-S, m^{-1}
β	activity coefficient related to adsorption energy, $mol^2\ kJ^{-2}$
C_0	initial concentration of phenol, mg L^{-1}
C_∞	equilibrium concentration of phenol, mg L^{-1}
C_{O_3}	ozone concentration, mg L^{-1}
$C_{O_3,L}$	ozone concentration in liquid, mg L^{-1}
$C^*_{O_3}$	concentration of ozone in the equilibrium with the ozone adsorbed on the activated carbon, mg L^{-1}
$C_{O_3,i}$	ozone concentration at the gas-liquid interface, mg L^{-1}
C_t	concentration of phenol at a given time t, mg L^{-1}
C_P	concentration of phenol in the liquid, mg L^{-1}
$C_{O_3,G}$	ozone concentration in the gas phase at the ozonator inlet, mg L^{-1}
$C^S_{O_3,i}$	ozone concentration in the liquid-solid interface, mg L^{-1}
C_{id}	amount of phenol adsorbed in a short period of time, mg g^{-1}
ε	Polyani potential
E	adsorption free energy per molecule, kJ mol^{-1}
E_a	activation energy, J mol^{-1}

ΔG	free energy changes, J mol^{-1}
He	Henry's constant, bar L mg^{-1}
ΔH	enthalpy change, J mol^{-1}
$k_{c,L}$	elemental kinetic constant for the ozonation in the liquid, L mg^{-1} min^{-1}
$k_{c,S}$	elemental kinetic constant for the ozonation in the solid, L mg^{-1} min^{-1}
K^*_G	ozone transfer constant for the whole process, mg bar^{-1} L^{-1} min^{-1}
K^*_L	global ozone transfer constant in the liquid including parallel reaction stages, mg bar^{-1} L^{-1} min^{-1}
K^S_L	global ozone transfer constant in the L-S interface, including the in-series reaction in the solid, mg bar^{-1} L^{-1} min^{-1}
K_G	global ozone transfer constant in the L-S interface, mg bar^{-1} L^{-1} min^{-1}
k_L	liquid-layer ozone transfer constant in the L-S interface, mg bar^{-1} m^{-2} min^{-1}
k_G	ozone transfer constant in the G-L interface, mg bar^{-1} m^{-2} min^{-1}
k_S	solid-layer ozone transfer constant in the G-L interface, mg bar^{-1} m^{-2} min^{-1}
k_{oxL}	kinetic constant of phenol oxidation referred to the liquid, min^{-1}
k_{oxS}	kinetic constant of phenol oxidation referred to the solid, (mg L^{-1})/(mg min g^{-1})
k_{ads}	kinetic constant of phenol adsorption, min^{-1}
K_F	Freundlich constant, (mg g^{-1}) (L mg^{-1})$^{1/n_F}$
K_L	Langmuir equilibrium constant, L mg^{-1}
k_1	pseudo first order rate constant, min^{-1}
k_2	pseudo second order rate constant, g mg^{-1} min^{-1}
k_{dif}	intraparticle diffusion rate constant, mg g^{-1} min$^{-0.5}$
k_0	frequency factor
m	slope of the equilibrium line between the liquid-solid phase
M	adsorbent mass, g
N_{O3}	whole ozone consumption: N_{O3}=N^{I}_{O3}+N^{II}_{O3}, mg L^{-1} min^{-1}
N^{I}_{O3}, N^{II}_{O3}	ozone consumption in the liquid, and in the solid, mg L^{-1} min^{-1}
n_F	heterogeneity factor, dimensionless
P_{O3}	partial pressure of ozone in the gas phase, bar
P^*_{O3}	partial pressure of the ozone in equilibrium with the adsorbed ozone on the solid, bar
$P_{O3,i}$	partial ozone pressure at the gas-liquid interface, bar
$P^{\wedge}_{O3}$	partial pressure of ozone in equilibrium with C^*_{O3}, bar
q_t	amount of phenol adsorbed at a time t, mg g^{-1}
q_∞	amount of phenol adsorbed onto activated carbon, mg g^{-1}
q_s	maximum amount of adsorbate that can be adsorbed on adsorbent, mg g^{-1}
Q_G	gas flow, L min^{-1}
R	universal gas constant, J mol^{-1} K^{-1}
R_i	initial adsorption amount, dimensionless
ΔS	entropy change, J mol^{-1} K^{-1}
T	temperature, K
t	time, min
V	volume of dissolution, L
w	activated carbon concentration, g L^{-1}
z	stoichiometric relation of the reaction between phenol and ozone
Z_{O3}	ozone concentration onto activated carbon, mg L^{-1}
$Z_{O3,i}$	ozone concentration in the liquid-solid interface, mg g^{-1}
Z_P	concentration of phenol in the solid, mg g^{-1}
$Z_{P,\infty}$	amount of phenol adsorbed in the solid in equilibrium, mg g^{-1}

Conflicts of interest

There are no conflicts of interest to declare.

Acknowledgements

The authors are grateful to the University of the Basque Country for their financial support of this study through the PPGA19/63 project and C. Ferreiro's predoctoral PIF grant (PIF16/367).

References

1 S. Nakayama, K. Esaki, K. Namba, Y. Taniguchi and N. Tabata, *Ozone-Sci. Eng.*, 1979, **1**, 119–131.
2 B. Wang, H. Zhang, F. Wang, X. Xiong, K. Tian, Y. Sun and T. Yu, *Catalysts*, 2019, **9**, 241.
3 I. Bartalis, I. Siminiceanu and E. Arany, *Rev. Chim.*, 2011, **62**, 1047–1051.
4 W. Cheng, X. Quan, R. Li, J. Wu and Q. Zhao, *Ozone-Sci. Eng.*, 2018, **40**, 173–182.
5 S. Gupta, G. Ashrith, D. Chandra, A. K. Gupta, K. W. Finkel and J. S. Guntupalli, *Clinical Toxicology*, 2008, **46**, 250–253.
6 O. US EPA, Phenol CAS 108-95-2, https://cfpub.epa.gov/ncea/iris2/chemicalLanding.cfm?substance_nmbr=88, (accessed July 2, 2019).
7 ECHA, CoRAP list of substances, https://echa.europa.eu/information-on-

chemicals/evaluation/community-rolling-action-plan/corap-list-of-substances, (accessed July 2, 2019).
8 H. Babich and D. L. Davis, *Regulatory Toxicology and Pharmacology*, 1981, **1**, 90–109.
9 Y.-P. Chiang, Y.-Y. Liang, C.-N. Chang and A. C. Chao, *Chemosphere*, 2006, **65**, 2395–2400.
10 Y. Z. Pi, J. Schumacher and M. Jekel, *Water Res.*, 2005, **39**, 83–88.
11 M. Sanchez-Polo, J. Rivera-Utrilla, G. Prados-Joya, M. A. Ferro-Garcia and I. Bautista-Toledo, *Water Res.*, 2008, **42**, 4163–4171.
12 M. A. Atieh, *APCBEE Procedia*, 2014, **10**, 136–141.
13 U. Jans and J. Hoigné, *Atmospheric Environment*, 2000, **34**, 1069–1085.
14 J. Rivera-Utrilla and M. Sanchez-Polo, *Appl. Catal. B-Environ.*, 2002, **39**, 319–329.
15 C. A. Zaror, *J. Chem. Technol. Biotechnol.*, 1997, **70**, 21–28.
16 J. Nawrocki, *Applied Catalysis B: Environmental*, 2013, **142–143**, 465–471.
17 F. J. Beltran, J. F. Garcia-Araya and I. Giraldez, *Appl. Catal. B-Environ.*, 2006, **63**, 249–259.
18 I. Sanchez, F. Stuber, J. Font, A. Fortuny, A. Fabregat and C. Bengoa, *Chemosphere*, 2007, **68**, 338–344.
19 F. Luck, *Catalysis Today*, 1999, **53**, 81–91.
20 M. C. Hidalgo, M. Maicu, J. A. Navío and G. Colón, *Catalysis Today*, 2007, **129**, 43–49.
21 D.-H. Han, S.-Y. Cha and H.-Y. Yang, *Water Research*, 2004, **38**, 2782–2790.
22 S. S. Sable, K. J. Shah, P.-C. Chiang and S.-L. Lo, *J. Taiwan Inst. Chem. Eng.*, 2018, **91**, 434–440.
23 R. Yi-fei, L. Han-jin, W. Chao-hai and L. Ling-feng, *J. Cent. South Univ. Technol.*, 2010, **17**, 300–306.
24 F. Lange, S. Cornelissen, D. Kubac, M. M. Sein, J. von Sonntag, C. B. Hannich, A. Golloch, H. J. Heipieper, M. Moeder and C. von Sonntag, *Chemosphere*, 2006, **65**, 17–23.
25 S. H. Lin and C. H. Wang, *Environ. Technol.*, 2003, **24**, 1031–1039.
26 X. Qu, J. Zheng and Y. Zhang, *J. Colloid Interface Sci.*, 2007, **309**, 429–434.
27 W. Pratarn, T. Pornsiri, S. Thanit, C. Tawatchai and T. Wiwut, *Chin. J. Chem. Eng.*, 2011, **19**, 76–82.
28 C. Ferreiro, N. Villota, J. I. Lombraña and M. J. Rivero, *Journal of Cleaner Production*, 2019, **228**, 1282–1295.
29 H. Valdes, M. Sanchez-Polo, J. Rivera-Utrilla and C. A. Zaror, *Langmuir*, 2002, **18**, 2111–2116.
30 P. M. Alvarez, J. Pablo Pocostales and F. J. Beltran, *J. Hazard. Mater.*, 2011, **185**, 776–783.
31 L. Lei, L. Gu, X. Zhang and Y. Su, *Appl. Catal. A-Gen.*, 2007, **327**, 287–294.
32 S. M. de A. Guelli Ulson de Souza, F. B. de Souza and A. A. Ulson de Souza, *Ozone-Sci. Eng.*, 2012, **34**, 259–268.
33 김환익, 문지훈 and J. Chung, *Journal of Korean Society of Environmental Engineers*, 2014, **36**, 311–316.
34 T. L. Silva, A. Ronix, O. Pezoti, L. S. Souza, P. K. T. Leandro, K. C. Bedin, K. K. Beltrame, A. L. Cazetta and V. C. Almeida, *Chem. Eng. J.*, 2016, **303**, 467–476.
35 O. E.-A. A. Adam, *American Chemical Science Journal*, 2016, **16**, 1–13.
36 R. J. Martin and W. J. Ng, *Water Research*, 1984, **18**, 59–73.
37 K. Sun, J. Jiang and J. Xu, *Iran J. Chem. Chem. Eng.-Int. Engl. Ed.*, 2009, **28**, 79–83.
38 X. He, M. Elkouz, M. Inyang, E. Dickenson and E. C. Wert, *J. Hazard. Mater.*, 2017, **326**, 101–109.
39 P. M. Álvarez, F. J. Beltrán, V. Gómez-Serrano, J. Jaramillo and E. M. Rodríguez, *Water Research*, 2004, **38**, 2155–2165.
40 C. Rodriguez, J. Ignacio Lombrana, A. de Luis and J. Sanz, *J. Chem. Technol. Biotechnol.*, 2017, **92**, 656–665.
41 Markandeya, S. P. Shukla and G. C. Kisku, *research Journal of Environmental Toxicology*, 2015, **9**, 320–331.
42 C. Ferreiro, N. Villota, J. I. Lombraña, M. J. Rivero, V. Zúñiga and J. M. Rituerto, *Water*, 2019, **11**, 337.
43 K. S. W. Sing, D. H. Everett, R. A. W. Haul, L. Moscou, R. A. Pierotti, J. Rouquerol and T. Siemieniewska, in *Handbook of Heterogeneous Catalysis*, ed. G. Ertl, Wiley-VCH Verlag GmbH & Co. KGaA, Weinheim, Germany, 2008.
44 A. Omri and M. Benzina, *Journalde la Société Chimique de Tunisie*, 2012, **14**, 175–183.
45 J. Lyklema, *Pure and Applied Chemistry*, 1991, **63**, 895–906.
46 H. Valdés and C. A. Zaror, *Ingeniare. Revista chilena de ingeniería*, 2010, **18**, 38–43.
47 C. Moreno-Castilla, *Carbon*, 2004, **42**, 83–94.
48 W. H. Brown, C. S. Foote, B. L. Iverson and E. Anslyn, *Organic Chemistry*, Cengage Learning, 2011.
49 C. VonSonntag and U. VonGunten, *Chemistry of Ozone in Water and Wastewater Treatment: From Basic Principles to Applications*, Iwa Publishing, London, 2012.
50 F. J. Beltran, *Ozone Reaction Kinetics for Water and Wastewater Systems*, CRC Press, 2003.
51 D. G. Argo, *Journal (Water Pollution Control Federation)*, 1980, **52**, 750–759.
52 F. A. Banat, B. Al-Bashir, S. Al-Asheh and O. Hayajneh, *Environmental Pollution*, 2000, **107**, 391–398.
53 G. Limousin, J.-P. Gaudet, L. Charlet, S. Szenknect, V. Barthès and M. Krimissa, *Applied Geochemistry*, 2007, **22**, 249–275.
54 S. Kaur, S. Rani and R. K. Mahajan, *Journal of Chemistry*, DOI:10.1155/2013/628582.
55 T. Allen, *Particle Size Measurement: Volume 2: Surface Area and Pore Size Determination.*, Springer Science & Business Media, 1996.
56 A. K. Meena, K. Kadirvelu, G. K. Mishraa, C. Rajagopal and P. N. Nagar, *J. Hazard. Mater.*, 2008, **150**, 619–625.
57 I. Enniya, L. Rghioui and A. Jourani, *Sustainable Chemistry and Pharmacy*, 2018, **7**, 9–16.
58 V. K. Gupta, S. Agarwal, H. Sadegh, G. A. M. Ali, A. K. Bharti and A. S. Hamdy Makhlouf, *Journal of Molecular Liquids*, 2017, **237**, 466–472.
59 Y. Ma, N. Gao, W. Chu and C. Li, *Frontiers of Environmental Science & Engineering*, 2013, **7**, 158–165.
60 Y. S. Ho and G. McKay, *Process Biochemistry*, 1999, **34**, 451–465.
61 S. Banerjee and M. C. Chattopadhyaya, *Arabian Journal of Chemistry*, 2017, **10**, S1629–S1638.
62 B. A. Fil, M. T. Yilmaz, S. Bayar and M. T. Elkoca, *Brazilian Journal of Chemical Engineering*, 2014, **31**, 171–182.
63 J. García Prieto, P. Pérez Galende, J. Manuel Cachaza Silverio and M. Roig, *Water Science & Technology: Water Supply*, 2012, **13**, 74.
64 N. R. C. (US) S. D. W. Committee, *An Evaluation of Activated Carbon for Drinking Water Treatment*, National Academies Press (US), 1980.
65 S. P. Ghuge and A. K. Saroha, *Journal of Environmental Management*, 2018, **211**, 83–102.
66 T. Nunoura, G. H. Lee, Y. Matsumura and K. Yamamoto, *Chem. Eng. Sci.*, 2002, **57**, 3061–3071.
67 C. Huang and H. Shu, *J. Hazard. Mater.*, 1995, **41**, 47–64.
68 H. Valdes, M. Sanchez-Polo and C. A. Zaror, *Latin American applied research*, 2003, **33**, 219–223.
69 M. E. Suarez-Ojeda, F. Stuber, A. Fortuny, A. Fabregat, J. Carrera and J. Font, *Appl. Catal. B-Environ.*, 2005, **58**, 105–114.
70 Y. Guo, L. Yang and X. Wang, *Journal of Environmental & Analytical Toxicology*, DOI:10.4172/2161-0525.1000150.
71 A. Fortuny, J. Font and A. Fabregat, *Appl. Catal. B-Environ.*, 1998, **19**, 165–173.

72 H. Delmas, C. Creanga, C. Julcour-Lebigue and A.-M. Wilhelm, *Chem. Eng. J.*, 2009, **152**, 189–194.
73 A. Rodríguez, R. Rosal, J. A. Perdigón-Melón, M. Mezcua, A. Agüera, M. D. Hernando, P. León, A. R. Fernández-Alba and E. García-Calvo, in *Emerging Contaminants from Industrial and Municipal Waste*, eds. D. Barceló and M. Petrovic, Springer Berlin Heidelberg, Berlin, Heidelberg, 2008, vol. 5S/2, pp. 127–175.
74 W. Xiong, N. Chen, C. Feng, Y. Liu, N. Ma, J. Deng, L. Xing and Y. Gao, *Environmental science and pollution research international*, DOI:10.1007/s11356-019-05304-w.
75 I. Quesada-Penate, C. Julcour-Lebigue, U. J. Jauregui-Haza, A. M. Wilhelm and H. Delmas, *J. Hazard. Mater.*, 2012, **221**, 131–138.
76 A. Eftaxias, J. Font, A. Fortuny, J. Giralt, A. Fabregat and F. Stuber, *Appl. Catal. B-Environ.*, 2001, **33**, 175–190.
77 E. Vega and H. Valdes, *Microporous Mesoporous Mat.*, 2018, **259**, 1–8.
78 T. Dutta, T. Kim, K. Vellingiri, D. C. W. Tsang, J. R. Shon, K.-H. Kim and S. Kumar, *Chemical Engineering Journal*, 2019, **364**, 514–529.
79 EPA, *United States Environmental Protection Agency*.
80 P.-J. Lu, H.-C. Lin, W.-T. Yu and J.-M. Chern, *Journal of the Taiwan Institute of Chemical Engineers*, 2011, **42**, 305–311.